

# Analysis on Overhead Shielded Coupling Effectiveness of Ring Seam by Matlab

Chun-jiang Shuai

Shanxi University of Technology, School of Physics and Electronic Information Engineering,  
Shanxi, Han zhong, 723001  
Email: huwewascj@163.com

**Abstract**—it was important to study the shielded effectiveness to reduce the electromagnetic interference and to protect electronic components. in this paper, the boundary element equation of linear segment was derived from the two-dimension boundary integral equation and linear interpolating function, and the formulas of potential and electric field intensity were also given. To demonstrate the accuracy and flexibility of the LBEM (linear boundary element method), the influence of the deformation degree of shielded deformed coaxial cable compared with the multipole theory on the results were discussed. Taking the overhead shielded coaxial cable and the overhead shielded two-core cable of ring seam as the research objects. The influences of ring seam in shielded effectiveness were analyzed by applying the LBEM with Matlab. The engineering example results showed that for overhead shield two-core cable, the change of coupling capacitance was related with the ring seam in deep layer of overhead shield two-core cable at the location of parallel core distance; and the change tendency of coupling capacitor with the ring seam at the vertical core distance was almost the same as the ring seam at the parallel core distance. But, when the ring seam depth was quite deep, very likely one core was exposed, and then the coupling capacitor decreased rapidly. Therefore the study of coupling effectiveness was instructive for more effective to defense EMI and will improve the overhead shielded cable electromagnetic compatibility.

**Index Terms**—Overhead shielded cable; Ring seam; Coupling capacitance; Linear boundary element method (LBEM); Matlab.

## I. INTRODUCTION

With the rapid development of China economy, the overhead coaxial cable and multi-core cable of copper were widely used in many important equipment connections, such as television, computer management system, fire fighting equipment, communications equipment, etc [1]. However, High-frequency components induced by high-speed signal transmission enable connection cables to produce substantial electromagnetic interference and leakage [2-4], in which the alien crosstalk originating from distributed capacitance and inductance leads to waveform distortion, increases bit error rate, and limits signal transmission distance [5]. Therefore, it was necessary to forecast the electromagnetic interference.

Overhead shielded cables [4] were over-ground cables laid high on utility poles. Although the insecure and aesthetically displeasing overhead cables were vulnerable to external influences, they were more easily laid and cost less compared to underground cables [6]. Therefore, overhead cables were still extensively applied in the cases of long distance, few users, frequent variations and underground cable laying difficulties. In addition to self-supporting cables, it was imperative to set messenger cables in the laying of overhead cables comprising less than 300 pairs of all-plastic cables which were prone to mechanical damages owing to the overwhelming dead weights. However, hanging overhead cables directly below messenger cables by iron wires that aim to lower costs as well as on-site barbaric constructions inevitably lead to circumferential welds[7, 8], which jeopardize the protection of shielding layers. As a result, electronic devices cannot normally function due to the disturbed signals upon external electromagnetic field excitation. Under extreme circumstances, the devices may even be devastated in the presence of high-power microwave pulses. The coupling capacitances of core wires in electronic devices could be determined only when parameters such as inductances and capacitances were given [9-11]. Thus, the coupling characteristics of the overhead communication cables containing circumferential weld shields must be studied to minimize the disturbances of electromagnetic waves.

At present, there were many studies on the shielded deformed cables, and the methods were varied, such as transmission line method [12], MOM [13], FDTD [5, 14] and Multi-pole theory [15]. However, the study on the influence of coupling capacitance effect of overhead shielded cable with ring seam. In this paper, with the overhead shielded coaxial cable and the overhead shielded two-core cable that had been unpublished as the research objects firstly, the influence of ring seam in shielded effectiveness were analyzed by applying the LBEM (linear boundary element method)[16-19] with Matlab[20-24]. To demonstrate the accuracy and flexibility of the LBEM, the influence of the deformation degree of shielded deformed coaxial cable compared with the multipole theory on the results were discussed. The engineering example results showed that for overhead shield two-core cable, the change of coupling capacitance

was related with the ring seam in deep layer of overhead shield two-core cable at the location of parallel core distance; and the change tendency of coupling capacitor with the ring seam at the vertical core distance was almost the same as the ring seam at the parallel core distance. But, when the ring seam depth was quite deep, very likely one core was exposed, and then the coupling capacitor decreased rapidly. Therefore the study was instructive for more effective to defense EMI and would improve the overhead shielded cable electromagnetic compatibility.

II. LINEAR BOUNDARY INTEGRAL EQUATION

A. Boundary Integral Equation

Two-dimension boundary integral equation was derived by Green's theorem [25]

$$C_p u(\vec{r}) = \int_{\Gamma_1} \left( G \frac{\partial u}{\partial n'} - g \frac{\partial G}{\partial n'} \right) d\Gamma + \int_{\Gamma_2} \left( qG - u \frac{\partial G}{\partial n'} \right) d\Gamma \tag{1}$$

Where  $G = -\frac{1}{2\pi} \ln|\vec{r} - \vec{r}'|$  was 2-dimension Green's function,  $\vec{r}$  was the vector of field point,  $\vec{r}'$  was the vector of field source,  $C_p$  was integral coefficient, which had related to the location of the field point, namely,

$$C_p = \begin{cases} 0 & p \text{ lies outside } \Omega \\ \theta/2\pi & p \text{ lies on } \Gamma \\ 1 & p \text{ lies inside } \Omega \end{cases} \tag{2}$$

Where  $\theta$  was angle of boundary  $\Gamma$  to field

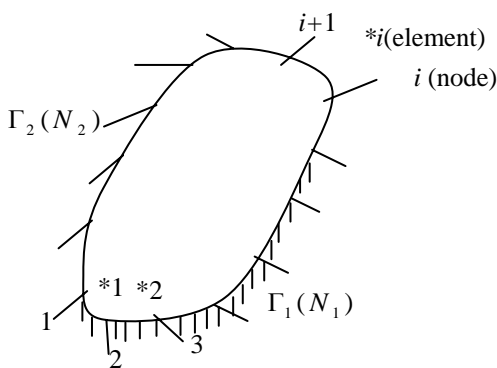


Fig.1 Line segment

$p$ . When  $p$  lies on  $\Gamma$ ,  $\theta = \pi$ ,  $C_p = 1/2$ .

In equation (1), if  $\vec{r} \in \Gamma$ , namely, the point of filed lies on boundary, then

$$C_p u_i = \int_{\Gamma_1} \left( G \frac{\partial u}{\partial n'} - g \frac{\partial G}{\partial n'} \right) d\Gamma + \int_{\Gamma_2} \left( qG - u \frac{\partial G}{\partial n'} \right) d\Gamma \tag{3}$$

This was the required integral equation. After boundary condition was given, uncertain variety  $u$  and  $\partial u / \partial n'$  on the boundary could be obtained by solving the equation, add to equation (1) then calculate the potential  $u$  and electric field intensity  $\vec{E} = -\nabla u$  of any point, that lies inside filed  $\Omega$ .

B. Linear Boundary Element Equation

Line segment of LBEM, as shown in Fig.1, boundary  $\Gamma_1(l_{k1})$  was discrete  $N_1$  line segments replace  $l_{k1}$ , and boundary  $\Gamma_2(l_{k2})$  was discrete  $N_2$  line segments replace  $l_{k2}$ ,  $N_1 + N_2 = N$ , these length of line segments can be different, each segment can be called a element(line segment is that each endpoint of boundary element was taken as node). Define the local coordinate

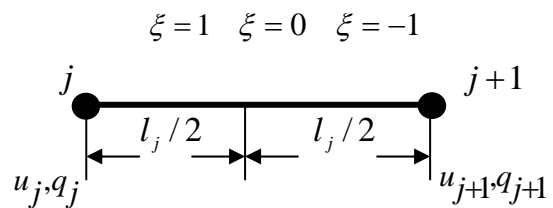


Fig.2  $u$  and  $q$  values on line segment in the local coordinate.

system of random No.  $j$  element ( $l_j$  was the length of element), the  $u$  and  $q$  value of any point in the element could be represented by the interrelated nodal values of  $u_j, u_{j+1}$  and  $q_j, q_{j+1}$  as well as the linear functions of  $\phi_1, \phi_2$  (interpolation basic function), as shown in Fig.2, namely

$$\begin{cases} u(\xi) = \phi_1 u_j + \phi_2 u_{j+1} = [\phi_1 \phi_2] \begin{bmatrix} u_j \\ u_{j+1} \end{bmatrix} \\ q(\xi) = \phi_1 q_j + \phi_2 q_{j+1} = [\phi_1 \phi_2] \begin{bmatrix} q_j \\ q_{j+1} \end{bmatrix} \end{cases} \tag{4}$$

Where  $\phi_1, \phi_2$  were interpolating radical function.

Add equation (4) to equation (3)

$$\begin{aligned}
 C_i u_i + \sum_{j=1}^{N_1+N_2} \begin{bmatrix} H_{ij}^{(1)} & H_{ij}^{(2)} \end{bmatrix} \begin{bmatrix} u_j \\ u_{j+1} \end{bmatrix} \\
 = \sum_{j=1}^{N_1+N_2} \begin{bmatrix} G_{ij}^{(1)} & G_{ij}^{(2)} \end{bmatrix} \begin{bmatrix} q_j \\ q_{j+1} \end{bmatrix}
 \end{aligned} \tag{5}$$

Where  $H_{ij}^{(2)} = \int_{l_j} \phi_2 \frac{\partial u^*}{\partial n'} dl$ ,

$$H_{ij}^{(1)} = \int_{l_j} \phi_1 \frac{\partial u^*}{\partial n'} dl,$$

$$G_{ij}^{(1)} = \int_{l_j} \phi_1 u^* dl,$$

$$G_{ij}^{(2)} = \int_{l_j} \phi_2 u^* dl$$

Equation (5) could be simplified by adding to required integral equation into the following equation, namely add equation (5) to equation (4), abbreviated formula was

$$\sum_{j=1}^N H_{ij} u_j = \sum_{j=1}^N G_{ij} q_j \tag{6}$$

Where  $H_{i,j} = \begin{cases} \hat{H}_{ij} & i \neq j \\ \hat{H}_{ij} + \frac{\theta}{2\pi} & i = j \end{cases}$

In equation (6), values of  $N_1 u_j$  on  $l_{k1}$  and  $N_2 q_j$  on  $l_{k2}$  were given by boundary condition, shown them with  $\bar{u}_0(N_1)$  and  $\bar{q}_0(N_2)$ ; values of  $N_1 \partial u / \partial n'$  on  $l_{k1}$  and  $N_2 u$  as uncertain variate, shown them with  $\bar{q}_1(N_1)$  and  $\bar{u}_1(N_2)$ . Then equation (7) could be expressed as the following block matrix

$$\begin{bmatrix} \bar{H}_0 & \bar{H}_1 \end{bmatrix} \begin{bmatrix} \bar{u}_0(N_1) \\ \bar{u}_1(N_2) \end{bmatrix} + \begin{bmatrix} \bar{G}_0 & \bar{G}_1 \end{bmatrix} \begin{bmatrix} \bar{q}_0(N_2) \\ \bar{q}_1(N_1) \end{bmatrix} = 0 \tag{7}$$

If the uncertain terms were put on the left of the equation, and the certain terms were put on the right of the equation, then equation (7) could be changed into the following:

$$\begin{bmatrix} \bar{H}_1 & \bar{G}_1 \end{bmatrix} \begin{bmatrix} \bar{u}_1(N_2) \\ \bar{q}_1(N_1) \end{bmatrix} = \begin{bmatrix} -\bar{G}_0 & -\bar{H}_0 \end{bmatrix} \begin{bmatrix} \bar{q}_0(N_2) \\ \bar{u}_0(N_1) \end{bmatrix} \tag{8}$$

Abbreviated formula was:

$$\bar{A} \bar{X} = \bar{B} \tag{9}$$

Where,  $\bar{A}$  was  $N \times N$  rank phalanx,  $\bar{X}$  and  $\bar{B}$  were  $N$  rank array. Equation (9) was the equation of linear boundary element method.

### III SHIELDED CABLE CAPACITANCE CALCULATION PRINCIPLE

#### A. Cable Capacitance Coupling Mechanism

Capacitive coupling was the electromagnetic interference phenomenon which caused by distributed capacitance between the electronic devices, electronic components, PCB line, and so on. The capacitance would be existed between the two conductors when they close to each other. And the conductive pathway would be formed through this reactance. This phenomenon was called capacitance coupling that the potential of other conductors were effect by the signals voltage (or noise voltage) of conductor through distributed capacitance, namely, electrostatic coupling or electrostatic induction.

The characteristic impedance  $Z_0$  of TEM transmission line as follows:

$$Z_0 = (\nu_0 C_0)^{-1}$$

Where,  $\nu_0 = 1/\sqrt{\mu\epsilon}$ , the capacitance  $C_0$  was computed at first. The signal would be reflex in the node of impedance discontinuity if the impedance of the transmission path had changed during the signal transmission. Thus, the changes of coupling capacitance were closely with electromagnetic interference, which would be affecting the quality of the signal transmission.

#### B. Shielded Cable Capacitance Calculation Principles

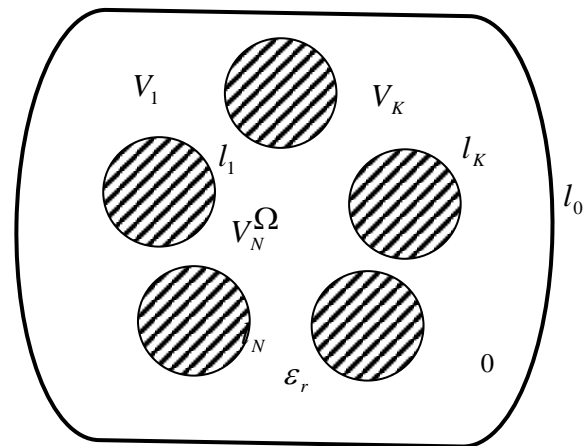


Fig.3 Various shielding cable

One of the main works of the electromagnetic compatibility analysis in the system was to calculate the capacitance coupling of guide line to core wire, thus, the coupling capacitance and free capacitance were computed at first. As shown in Fig.3, assume the shielded structure (conductor 0) was zero potential conductors, and the potentials of the other  $N$  conductors were respectively  $V_1, V_2, \dots, V_N$ , then the boundary value problems of electrostatic field as follows

$$\begin{cases} r \frac{\partial}{\partial r} (r \frac{\partial u}{\partial r}) + \frac{\partial^2 u}{\partial \theta^2} = 0, r, \theta \in \Omega \\ u|_{l_0} = 0, u|_{l_1} = V_1, u|_{l_2} = V_2, \dots, u|_{l_N} = V_N \end{cases} \quad (10)$$

Where  $\Omega$  was field,  $l_k$  was  $k$  conductor boundary curve of  $k$  conductor,  $V_k$  was  $k$  conductor potential.

The capacitance matrix of shielded multi-conductor cable was

$$\begin{bmatrix} \lambda_1 \\ \lambda_2 \\ \vdots \\ \lambda_N \end{bmatrix} = \begin{bmatrix} C_{11} & C_{12} & \dots & C_{1N} \\ C_{21} & C_{22} & \dots & C_{2N} \\ \vdots & \vdots & \vdots & \vdots \\ C_{N1} & C_{N2} & \dots & C_{NN} \end{bmatrix} \begin{bmatrix} V_1 \\ V_2 \\ \vdots \\ V_N \end{bmatrix} \quad (11)$$

Where  $C_{ii} = (\lambda_i / V_i)|_{V_i=V_0, V_j=0}$  were free capacitances,  $C_{ij} = (\lambda_i / V_j)|_{V_j=V_0, V_i=0(i, j=1, 2, \dots, N; i \neq j)}$  were coupling capacitance.

C. Matlab Introduction [26]

Matlab was both a powerful computational environment and a programming language that easily handles matrix and complex arithmetic. It was a large software package that has many advanced features built-in, and it had become a standard tool for many working in science or engineering disciplines. Among other things, it would allow easy plotting in both two and three dimensions.

Matlab had two different methods for executing commands: interactive mode and batch mode. In interactive mode, commands are typed (or cut-and-pasted) into the 'command window'. In batch mode, a series of commands were saved in a text file (either using Matlab's built-in editor, or another text editor such as Emacs) with a '.m' extension. The batch commands in a file were then executed by typing the name of the file at the Matlab command prompt. The advantage to using a '.m' file was that you could make small changes to your code (even in different Matlab sessions) without having to remember and retype the entire set of commands. Also, when using Matlab's built-in editor, there were simple debugging tools that can come in handy when your programs start getting large and complicated. More on writing .m files later.

IV. ANALYZED RESULTS

A. Comparison of Theory and the Multi-pole Theory

As shown in Fig.4[16], two dimension multi-boundary condition, stationary solution as follows:

$$\left. \begin{cases} \nabla^2 u = 0 & \in \Omega \\ u|_{x=0, 0 \leq y \leq b} = 0 \\ u|_{y=b, 0 \leq x \leq a} = 0 \\ \frac{\partial u}{\partial n'}|_{y=0, 0 \leq x \leq a} = 0 \\ u|_{x=a, 0 \leq y \leq b} = 1.0V \end{cases} \right\} \quad (12)$$

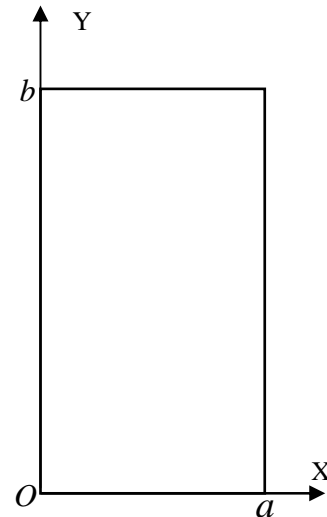


Fig. 4 Two dimension multi-boundary condition.

TABLE. I

COMPARISON OF THE CALCULATION RESULTS OF ELECTRIC FIELD INTENSITY WITH THEORETICAL VALUE (UNIT: V/M)

Coordinat e (m)		Theoretical value		Paper (LBEM)	
x	y	-E <sub>x</sub>	E <sub>y</sub>	-E <sub>x</sub>	E <sub>y</sub>
0.5	2.0	0.469	0.02	0.4694	0.02
		4	87		87
1.0	2.0	0.498	0.04	0.4982	0.04
		1	31		31
1.5	2.0	0.530	0.03	0.5306	0.03
		6	21		24
1.0	0.5	0.500	0.00	0.5000	0.00
		0	32		32
1.0	1.0	0.499	0.00	0.4999	0.00
		9	86		86
1.0	1.5	0.499	0.01	0.4996	0.01
		6	95		95
1.0	2.5	0.491	0.09	0.4911	0.09
		1	39		39
1.0	3.0	0.458	0.19	0.4586	0.19
		6	93		93
1.0	3.5	0.327	0.37	0.3279	0.37
		9	75		75

By the above method, the rectangular boundary would be subdivided for the 188 linear segments, which the four

boundary of angle would be subdivided for 72 linear segments after treatment smooth according to the power function. By the general program of LBEM, the following calculation results of electric field intensity was obtained, as illustrated in TABLE. I .

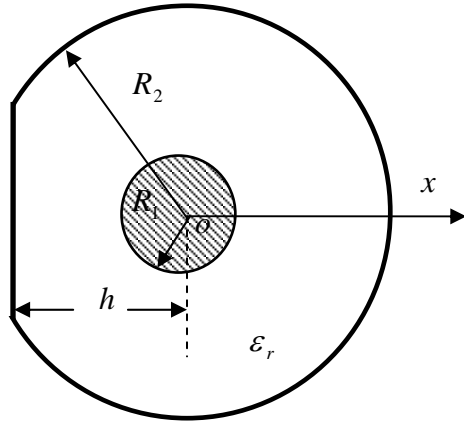


Fig.5 Shielded deformed coaxial cable

See TABLE. I , the calculation results of electric field intensity were well in agreement with the theoretical value, where the maximum relative error was only 0.02%, that precision was greatly improved better than double-angle method (the maximum relative error is 0.36%). Therefore, LBEM precision was quite high.

The shielded deformed coaxial cable as shown in Fig.5 [15], the cables easily lead to deformed in practice, when placed on the ground for long times due to gravity and the friction between the surface. The parameters:  $R_1 = 0.455\text{mm}$ ,  $R_2 = 1.49\text{mm}$ ,  $\epsilon_r = 2.03$ ,  $\mu_r = 1$ . By the general program of linear boundary element method, the following calculation results of shielded deformed coaxial cable about capacitor were obtained, as illustrated in TABLE. II .

TABLE. II

COMPARISON OF THE CALCULATION RESULTS OF THE SHIELDED DEFORMED COAXIAL CABLE WITH THE MULTIPOLE THEORY VALUE (PF)

$h/mm$	0.5	0.6	0.7	0.8	0.9	1.0
$C_{LBEM}$	269.9	164.0	134.2	119.5	110.8	105.1
$C_{MT}$	269.1	164.5	134.4	119.6	110.8	105.1
$h/mm$	1.1	1.2	1.3	1.4	1.45	
$C_{LBEM}$	101.2	98.55	96.78	95.64	95.31	
$C_{MT}$	101.2	98.51	96.72	95.60	95.28	

As shown in TABLE. II , the calculation results of shielded deformed coaxial cable about capacitor were well in agreement with the multipole theory value [15], where the maximum deviation is only 0.3%, and the capacitor increased with the deformation degree of the shielded deformed coaxial cable.

*B. Overhead Shielded Cable Coupling Capacitance Calculation*

Overhead shield coaxial cable of ring seam as shown in Fig.6, which were consisted of one cylindrical conductors and shielded shell. The parameters: conductor number\* section ( $\text{mm}^2$ ) =  $1 \times 0.322 \text{ mm}^2$ ,  $R = 1.86\text{mm}$ ,  $d$  was the ring seam depth of shield shell, the dielectric constant  $\epsilon_r = 2.33$ .

As shown in Fig.7, the capacitor of ring seam in overhead shield coaxial cable varied with the ring seam depth of shield shell by applying the LBEM with Matlab was given. See Fig.7, when the ring seam was in the shallow shell, the capacitor of ring seam on overhead

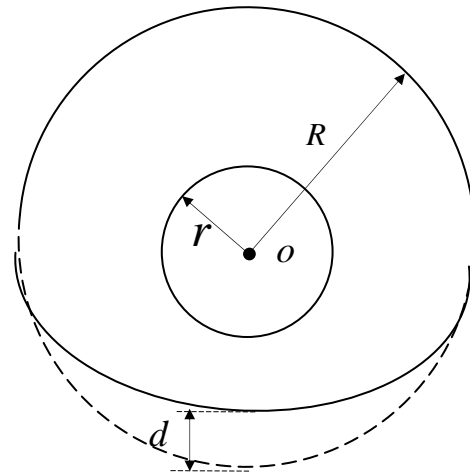


Fig.6 Overhead shield coaxial cable of ring seam

shield coaxial cable had little change, while when the ring seam depth was greater than 0.5 mm, the capacitor changed greatly.

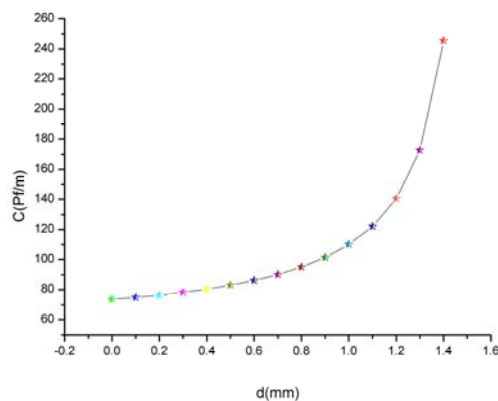


Fig.7 Capacitor of shield coaxial cable of ring seam varied with d

As shown in Fig.8, overhead shield two-core cable of ring seam was consisted of 2 cylindrical conductors and shielded conductor. The parameters: conductor number\* section ( $\text{mm}^2$ ) =  $2 \times 0.322 \text{ mm}^2$ ,  $R = 1.86\text{mm}$ , core distance =  $2 \times 0.64 \text{ mm}$ ,  $d$  was the ring seam depth of shield shell, the dielectric constant  $\epsilon_r = 2.33$ , filling

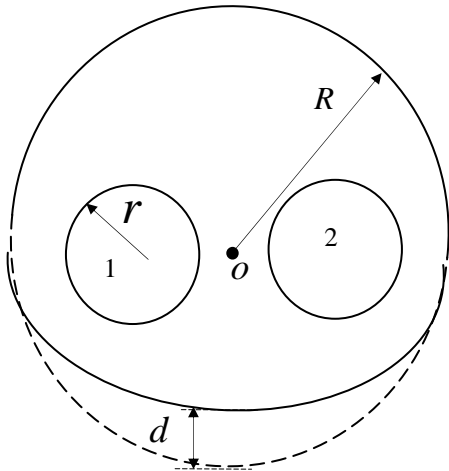


Fig.8 Overhead shield two-core cable of ring seam

medium was xlpe between the shielded shell with core.

As shown in Fig.9, the coupling capacitor of ring seam in overhead shield two-core cable varied with  $d$  at the location of parallel core distance was given. The coupling capacitor decreased greatly with the depth of ring seam increasing, so the cable signal transmission quality would have a great effect on the ring seam.

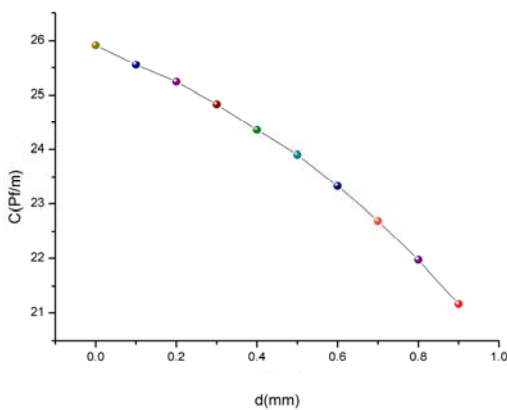


Fig.9 Coupling capacitor of shield coaxial cable of ring seam varied with  $d$  at location of parallel core distance

When at the location of vertical core distance near the core 2, the even mode capacitor of ring seam in overhead shield two-core cable varied with  $d$  was given. As shown in Fig.10,  $C_1$ 、 $C_2$  was even mode capacitor of core 1 and core 2.  $C_1$  had little change with the ring seam depth increasing ;but  $C_2$  had change greatly with the ring seam depth increasing, especially, when the ring seam depth

was greater 0.4mm, the even mode capacitor of core 2 ( $C_2$ ) increased greatly.

As shown in Fig.11, the coupling capacitor of ring

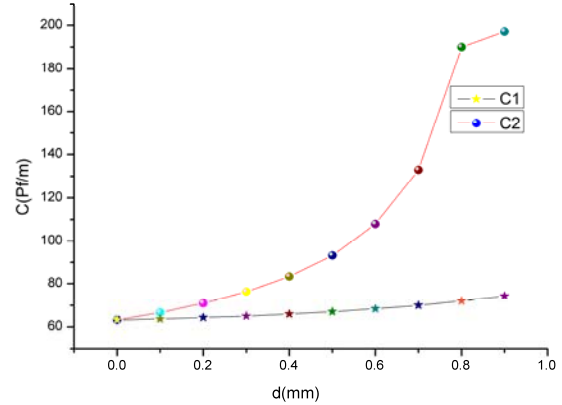


Fig.10 Even mode capacitor of shield coaxial cable of ring seam varied with  $d$  at location of vertical core distance

seam in overhead shield two-core cable varied with  $d$  at the location of vertical core distance was given. The change tendency of coupling capacitor with the ring seam at the vertical core distance was almost the same as the ring seam at the parallel core distance. Especially, when the ring seam depth was at 0.9mm (namely, the core 2 was exposed), the coupling capacitor decreased rapidly.

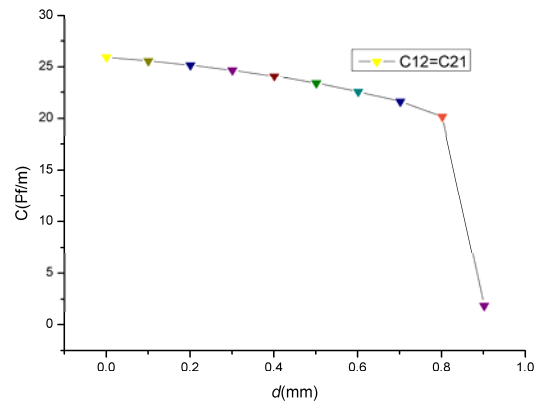


Fig.11 Coupling capacitor of shield coaxial cable of ring seam varied with  $d$  at location of vertical core distance

CONCLUSIONS

The boundary element equation of linear segment was discrete from linear interpolating approximation, which was applied to deal with the problem of 2-dimensional electrostatic field, such as two dimension multi- boundary condition and shielded deformed coaxial transmission lines, and it shows this method is effective and feasible through numerical examples. This method not only solves the discontinuous problem, but also the precision of the

method was high. For the overhead shield coaxial cable of ring seam and the overhead shield two-core cable of ring seam that not had been published, this paper provides coupling capacitor of these cable by this method for the first time. It had been shown that this method is provided with a great deal of merits such as simple operation and convenient calculation, so it would be have fine general availability.

(1) This paper proposed to use linear boundary element method to deal with the capacitor of ring seam which was set in shielded shell by Matlab, such as overhead shield coaxial cable, overhead shield two-core cable.

(2) The ring seam had become one of the main causes for reduction the cable shielded effectiveness. The analysis on the shielded effectiveness of overhead communication cables with ring seam showed that the capacitance of overhead shield coaxial cable of ring seam varied scarcely if the ring seam was in shallow layer, the capacitor changed greatly when the ring seam depth was greater than 0.5 mm; and the change of coupling capacitance was related with the ring seam in deep layer of overhead shield two-core cable at the location of parallel core distance.

The change tendency of coupling capacitor with the ring seam at the vertical core distance was almost the same as the ring seam at the parallel core distance. And, when the ring seam depth was at 0.9mm (namely, one core was exposed), the coupling capacitor decreased rapidly.

(3)Therefore, the electrical workers should use the supporter rather than use a wire to hold the cable simply during set up the overhead shield cable, and then the signal transmission can be guaranteed.

(4)The coupling effect of any one multi-core cable and different sections cable would be analyzed by the linear boundary element method.

#### ACKNOWLEDGMENT

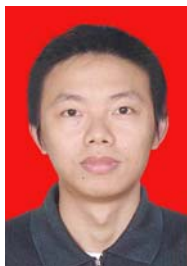
Project: the Science and Technology Program of the Education Department of Shaanxi Province Government (number: 09JK378); the Key Scientific Research Foundation of Shaanxi University of Technology (number: SLGKY12-02).

#### REFERENCES

- [1] LIU ZY. *Ultra-high voltage grid* [M]. Beijing: Chinese Economic Press, 2005, pp .1-20.
- [2] ZHENG JQ. *EMC design and test cases analysis* [M]. Beijing: Electronics Industry Press, 2006, pp .2-3.
- [3] ZHENG BY, SHEN ZX. *Shielding Effectiveness of Cylindrical Enclosures with Rectangular Apertures [A].2008, Asia-Pacific Symposium on Electromagnetic Compatibility and 19th International Zurich Symposium on Electromagnetic Compatibility*[C].Singapore, 2008,pp.710-713.
- [4] WANG J, ZHANG XQ, WAQNG T, etc. *Influence of 50Hz electric field generated by AC high-voltage overhead power lines on human body*[J]. *Advanced Technology of Electrical Engineering and Energy*, 2011(3), pp .43-46.
- [5] MA F,ZHU ZP,QIAN Bao-liang,etc. *Investigation on Multi-Peak Resonant Characteristic of Microwave Coupling into the Cavity with a Narrow Rectangular Slot* [J]. *Journal of Microwaves*, 2008, 24(S1),pp.40-43.
- [6] LIANG YC, CAI JA, LI YM, etc. *Calculation of amp city reduction factors for buried cables with surroundings based on FEM* [J].*Advanced Technology of Electrical Engineering and Energy*, 2007(4), pp .10-13.
- [7] LIU SQ, FU JM, ZHOU H, etc.*Numerical studies on coupling effects of EMP into slots* [J]. *Chinese Journal of Radio Science*,1999,14(2), pp.202-206.
- [8] XIAO JS, LIU WH, ZHANG SY, etc. *Numerical simulation on coupling effects of ultra wide band electromagnetic pulse into slots in a cavity*[J].*High Power Laser &Particle Beams*,2010 ,22(12), pp .2959—2963.
- [9] SHI PF.*Study on the Coupling Efects of Ultra-wide Spectrum Electromagnetic Pulse to the Hole that Passing through the Shield* [D]. Lanzhou: Lanzhou University,2010.
- [10] SHUAI CJ. *Analysis on Shielding Effectiveness of Rural Concealed Communication Cable of Asymmetric and Symmetric Slots with Different Shapes*[J].*Agricultural Science & Technology*,2012,13(8),pp.1781-1783.
- [11] Benahmed N, Feham M. *Finite element analysis of RF couplers with sliced coaxial cable*[J].*Microwave Journal*,2000,43(11), pp .106—120.
- [12] YI B. *Research on the Law of Electromagnetic Pulse Coupling to the Shield Cable*[D].Beijing: North China Electric Power University,2008.
- [13] Cerri G, De Leo R, Primiani V M. *Theoretical and experimental evaluation of the electromagnetic radiation from apertures in shielded enclosures*[J].*IEEE Trans on Electromagnetic Compatibility*,1992,34(11),pp.423-432.
- [14] Teppati V, Goano M, Ferrero A. *Conformal-mapping design tools for coaxial couplers with complex cross section*[J].*IEEE Trans*,2002, MTT-50(12), pp .2339—2345.
- [15] ZHENG QH,XIE FY,CAI WD.*Multipole theory analysis on the capacitance of shielded multi-conductor cable*[J].*High Power Laser &Particle Beams*,2003,15(10), pp .999—1002.
- [16] SHUAI CJ. *Analysis of linear boundary element angle problem with angle arc method* [C].*Proc. of SPIE*, 2009(7512), pp, 75120H-1—75120H-7.
- [17] SHUAI CJ, *The Mixed Method Analysis of Higher Order Mode in Waveguide of Piecewise Homogeneous Dielectric* [J]. *Applied Mechanics and Materials*, 2012 (Vols. 134), pp .3334-3337.
- [18] SHUAI CJ., Li RM. *The linear boundary element method of calculating the problems of transmission line about piecewise homogeneous dielectric* [J].*Journal of Shaanxi University of Technology (Natural Science Edition)*.2008, 24(4), pp, 61-66.
- [19] SHENG JN. *Numerical analysis of electromagnetic fields project* [M].Sian: Press of Xi'an Jiaotong University, 1991.
- [20] SHUAI CJ. *Analysis on the 2D Electrostatic Field of Polygon Groove by MATLAB* [J].*Journal of Shaanxi University of Technology (Natural Science Edition)*.2012, (1), pp .59-62.
- [21] Li RM, Zhang JS. *The professional technicians performance appraisal of coal mine* [J].*Coal Technology*, 2011(7), pp.249-251.
- [22] Li RM. *Analysis on management object classification with cluster analysis method by Matlab* [J].*China High Technology Enterprises*, 2010(27), pp.128-129.
- [23] Zhang XM, Li Y. *Improving SVM through a Risk Decision Rule Running on MATLAB*[J].*Software*

Application for Economic Analysis and Business Management,2012,10(7),pp, 2252-2257.

- [24] Li SHQ,He L.*Co-simulation Study of Vehicle ESP System Based on ADAMS and MATLAB*[J].Software Application for Economic Analysis and Business Management,2011,6 (5),pp,866-872.
- [25] Li Z Y. *Electromagnetic field boundary element method* [M].Beijing: Press of Beijing Institute of Technology, 1987.
- [26] *Matlab Introduction*,Retrieved October 12,2007,from the World Wide Web:  
[Http://www.owl.net.rice.edu/~elec241/matlab.html](http://www.owl.net.rice.edu/~elec241/matlab.html).



**SHUAI Chun-jiang**(1979-),male, ,born in Jiangxi yichun, lecturer, major: computer-aided calculation and optimization design of electric machines.  
E-mail:huweiscj@163.com.